Journal of the Korean Chemical Society
2024, *Vol. 68, No. 2*
Printed in the Republic of Korea
https://doi.org/10.5012/jkcs.2024.68.2.82

Solid-State Ball-Mill Synthesis of Prussian Blue from Fe(II) and Cyanide Ions and the Influence of Reactants Ratio on the Products at Room Temperature

Youngjin Jeon

Department of Applied Chemistry, College of Science and Technologies, Konkuk University
268 Chungwondae-ro, Chungju 27478, Korea. E-mail: jeonyj@kku.ac.kr
(Received January 5, 2024; Accepted February 24, 2024)

ABSTRACT. This paper presents the solid-state synthesis of insoluble Prussian blue ($Fe_4[Fe(CN)_6]_3 \cdot xH_2O$, PB) in a ball mill, utilizing the fundamental components of PB. Solid-state synthesis offers several advantages, such as being solvent-free, quantitative, and easily scalable for industrial production. Traditionally, the solid-state synthesis of PB has been limited to the reaction between iron(II/III) ions and hexacyanoferrate(II/III) complex ions, essentially an extension of the solution-based co-precipitation method to solid-state reaction. Taking a bottom-up approach, a reaction is designed where the reactants consist of the basic building blocks of PB: Fe^{2+} ions and CN^- ions. The reaction, with a molar ratio of Fe^{2+} and CN^- corresponding to 1:2.8, yields PB, while a ratio of 1:6.6 results in a mixture of potassium hexacyanoferrate(II) ($K_4Fe(CN)_6$), potassium chloride (KCl), and potassium cyanide (KCN). This synthetic approach holds promise for environmentally friendly methods to synthesize multimetallic PB with maximum entropy in nearly quantitative yield.

Key words: Prussian Blue, Solid-state synthesis, Ball-mill synthesis, Bottom-up approach, Nanocrystalline materials.

INTRODUCTION

Prussian Blue (PB, $Fe_4[Fe(CN)_6]_3 \cdot xH_2O$), a widely-used pigment in art and dyeing, is a coordination compound with a fascinating history of discovery and application.[1] In recent years, PB and its analogs (PBAs) have been widely studied compounds due to their interesting electrochemical,[2] catalytic,[3] optical,[4] and magnetic properties.[5] Various synthetic methods for Prussian Blue and PBAs have been developed to obtain the suitable PB for a specific application, including the co-precipitation, single-source, and dual-source methods. The co-precipitation method, commonly used for synthesizing PB and PBAs, involves using bare metal ions and a hexacyanometalate as reactants mixed in a suitable solvent, usually an aqueous solution.[6,7] Another popular method is the single-source method, utilizing a single precursor, a hexacyanoferrate(II/III) or hexacyanocobaltate(III). The presumed mechanism involves acid-catalyzed hydrolysis and a subsequent reaction with an unhydrolyzed hexacyanoferrate ion, yielding monometallic PB or PBAs with high purity and control over stoichiometry and morphology.[8,9] The dual-source method can be used to synthesize bimetallic PBAs, involving two different hexacyanometalate precursors mixed in an acidic aqueous solution under elevated temperatures.[10,11] This method offers flexibility in the choice of metal ions and stoichiometry, requiring careful optimization of reaction conditions for a pure product with desired properties.

In addition to solution-based synthesis, solid-state PB synthesis is gaining attention due to advantages such as not requiring a solvent, high reproducibility with near-quantitative yields, versatility in synthesizing various PBAs, and scalability for industrial production. The major method for solid-state PB synthesis is the ball-milling technique, involving the grinding of reactants in a ball mill to facilitate the reaction. The solid-state PB synthesis is largely limited to a method like the co-precipitation method in the solution.[11-15] In this approach, metal ions and hexacyanometalate in the solid state are mixed to form PBAs with the connectivity of CN^- groups retained as follows:

$$yM^{x+}(s) + xM'(CN)_6^{y-}(s) \rightarrow M_y[M'(CN)_6]_x \cdot nH_2O(s) \quad (1)$$

Regarding the connectivity of CN^-, M is coordinated to the N of CN^-, whereas M' is coordinated to the C of CN^-. However, there have been no reported solid-state syntheses of PB or PBAs using the most basic components of PB, iron ion species, and cyanide ions. This novel approach provides greater flexibility in selecting the metal ion species and the control of connectivities of CN^- ligands, yielding a product with "maximum entropy."

In this paper, an innovative solid-state synthesis method for PB using ball-milling, employing the fundamental building blocks of Fe^{2+} and CN^- as the reactants is suggested. The resulting product was determined through meticulous

control of the molar ratio of the reactants, and they are characterized by employing various techniques such as X-ray diffraction, Fourier-transform infrared (FT-IR) spectroscopy, and field-emission scanning electron microscopy (FE-SEM).

EXPERIMENTAL

All the reagents were purchased from commercial sources and used without further purification. The diffraction patterns were collected from 10° to 90° at a scan rate of 5°/min with Cu K_a radiation (40 kV and 30 mA) with a step size of 0.02° on a Rigaku MiniFlex diffractometer (Rigaku Corporation, Japan). Fourier transform infrared (FT-IR) spectra were recorded using a Nicolet iS5 FT-IR spectrometer (Thermo Fisher Scientific Inc., Waltham, MA, USA). Ball-mill syntheses were conducted with an LM-BD4530 ball-mill with a zirconia-lined jar (LKlab Korea, Seoul, Korea). Scanning electron micrographic images were obtained with a JSM-IT800 FE-SEM spectrometer (JEOL, Japan). Deionized water was purified on a new P.Nix UP 900 water purification system with a resistivity of 18.3 MW·cm (Human Corporation, South Korea). The reagents used in the reaction include iron(II) chloride tetrahydrate ($FeCl_2·4H_2O$ CAS No.:13478-10-9) and potassium cyanide (KCN, CAS No.: 151-50-8).

Synthesis of PB (1, 2, and 3)

To synthesize products **1** and **2**, a zirconia-lined ball-mill jar filled with approximately 30 zirconia balls with a diameter of 10 mm was charged with 10.916 g (54.9 mmol) of iron(II) chloride tetrahydrate ($FeCl_2·4H_2O$) and 10.108 g (155 mmol) of potassium cyanide (KCN) without (sample **1**) and with (sample **2**) a drop of conc. HCl. The reaction mixture was ball-milled at 35 rpm for 72 h, followed by the addition of 500 mL of 0.1 M HCl to the ball-mill jar and another 10 min of ball-milling to wash out the unreacted metal ions and metal oxides. The resulting mixture was filtered and washed with deionized water and EtOH several times. The power resultant was subsequently dried overnight in an oven (60 ℃). Product **3** was synthesized with the same method as reaction **2** except for the reactant ratio (Fe^{2+}:CN^- = 1:6.6). The resulting product was directly isolated from the ball-mill jar after the reaction and used for the analysis with XRD and FT-IR.

XRD Pattern Acquisition

The sample was prepared by the solid-state reaction and used as dried in an oven. Powder X-ray diffraction data were collected at room temperature using a Rigaku Mini-Flex diffractometer (Rigaku Corporation, Japan) with Cu K_a radiation. The diffraction data were collected over a 2θ range of 10-90° with a step size of 0.02° and a counting time of 1 second per step.

RESULTS AND DISCUSSION

As a proof of concept, the synthesis of PB using the reactants Fe^{2+} and cyanide (CN^-) ions in a ball mill without any added chemical reagents or solvent. The reaction is expressed as follows:

$$7\ Fe^{2+}(s) + 18\ CN^-(s) \rightarrow Fe_4[Fe(CN)_6]_3 \cdot xH_2O(s) \quad (2)$$

Typically, insoluble PB, expressed with the formula $Fe^{III}_4[Fe^{II}(CN)_6]_3 \cdot xH_2O$ with varying values of x up to 16, has a molar ratio of $Fe^{II/III}$:CN^- equal to 7:18, or 1:2.57. In one reaction, iron(II) chloride tetrahydrate ($FeCl_2·4H_2O$) and potassium cyanide (KCN) were employed, and their molar ratio was adjusted to 1:2.83, in which 2.83 is equivalent to 1.1 eq. of 2.57 ratio of CN^- (sample **1**). This slight excess of CN^- was introduced to potentially safeguard against the generation of unreacted iron species in case of a shortage of CN^- ions. In a subsequent reaction, the conditions mirrored those of the preceding one, with the sole exception being the introduction of a drop of concentrated HCl. This addition, corresponding to a small amount, was implemented to deter the formation of iron oxide species (sample **2**). Hereafter, samples without and with the addition of a drop of concentrated HCl will be referred to as sample **1** and sample **2**, respectively. The typical ball mill synthesis was conducted at 35 rpm for 72 hours to ensure the completion of the reaction.

After the reactions, samples **1** and **2** commonly exhibit a dark blue color with a powdery nature, both of which are non-dispersible in water. They were washed with 1 M HCl solution, distilled water, and ethanol several times to eliminate by-products such as the minute unreacted metal ions, metal oxide, or potassium cyanide that might be formed during the reaction. The appearances of the products are almost indiscernible from each other. Surprisingly, the percent yields of both products amount to *ca.* 98% based on the added iron chloride tetrahydrates. The structures of the crystalline products were examined with a powder X-ray diffraction (XRD) and analyzed with Rietveld refinement as shown in *Fig*. 1. The results of Rietveld refinement are shown in *Table* 1. The patterns match well with the previously reported pattern (JCPDS No. 01-073-0689).[16] Sample **1** reveals that the structure has a face-centered cubic

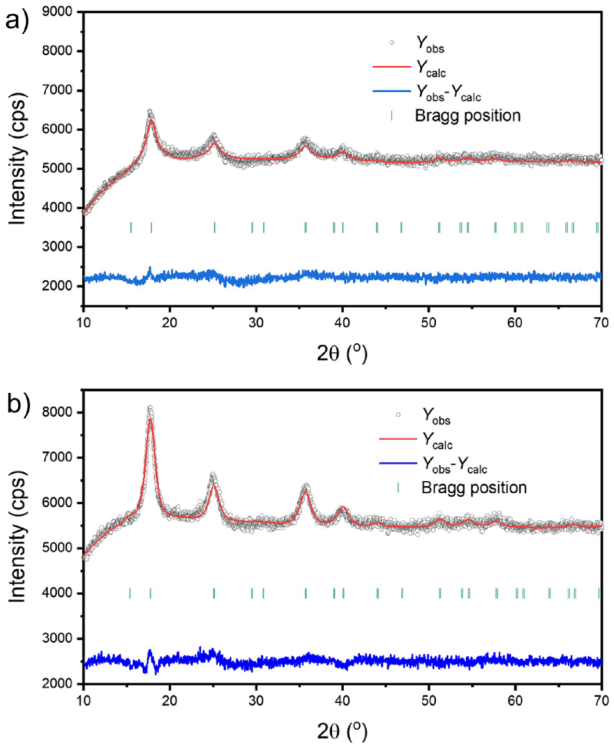

***Figure* 1.** XRD patterns and Rietveld refinement of (a) sample **1** and (b) sample **2**, respectively.

***Table* 1.** Summary of Crystallographic Parameters for **1** and **2**

	Sample **1**	Sample **2**
MW, g/mol	1095.2	1095.2
a, Å	10.18(1)	10.121(7)
α, deg	90	90
V, Å^3	1054.82	1036.69
Z	4	4
space group	*Fm*-3*m* (225)	*Fm*-3*m* (225)
ρ_{calc}, g/cm^3	1.7239	1.7540
R_{wp} [a,b]	1.380	1.366
R_{exp} [b,c]	1.378	1.329
T, K	298	298
GOF (R_{wp}/R_{exp})	1.0024	1.0562

[a] $R_{wp} = \{[\Sigma_i w_i(y_i^{calc} - y_i^{obs})^2]/[\Sigma_i w_i(y_i^{obs})^2]\}$. [b] y_i^{calc} and y_i^{obs} are the calculated and observed intensities at the *i*th point in the profile, normalized to monitor intensity. The weight w_i is $1/\sigma^2$ from the counting statistics, with the same normalization factor. *N* is the number of points in the measured profile minus the number of parameters. [c] $R_{exp} = \{N/[\Sigma_i w_i(y_i^{obs})^2]\}^{1/2}$.

phase with a lattice constant of $a = 10.18(1)$, with characteristic peaks at $2\theta = 17.85°$, 25.15°, 35.76°, and 40.00° in the XRD pattern. Sample **2** also exhibits the same phase as reaction **1** with a lattice constant of $a = 10.121(8)$. Goodness-of-fits of both compounds converge close to 1, which reveals the coincidence of the structure with the diffraction patterns. Compared to sample **1**, sample **2** exhibits more crystallinity estimated from the higher intensity, which reflects that adding HCl might enhance the crystallinity of the products.

To investigate the crystallite sizes of the products from the XRD patterns, Debye-Scherrer[17] and Williamson-Hall (W-H) analyses[18] were carried out, and the two results were compared. The Debye-Scherrer equation, $D = K\lambda/\beta\cos\theta$, is used to calculate the crystalline size of the nanoparticles, where D is the crystalline size of nanoparticles, K represents the Scherrer constant (0.98), λ denotes the wavelength (1.5406 Å) of X-ray, and β denotes the full width at half maximum (FWHM) of the chosen peak. Debye-Scherrer analyses were performed on a peak corresponding to the (002) plane with the highest intensity of all the peaks of samples **1** and **2** to estimate the crystallite size to be 5.42 nm and 8.03 nm, respectively. W-H analysis is a simplified integral breadth method where both size-induced and strain-induced broadening are deconvoluted by considering the peak width as a function of 2θ as shown below.[18]

$$\beta_T \cos\theta = \varepsilon(4\sin\theta) + K\lambda/D \quad (3)$$

where β_T is the full width at half maximum of the diffraction peaks, e is the microstrain, θ is the Bragg angle, K is 0.98 for the nanocrystalline compounds, λ is the wavelength of X-rays, and D is the crystallite size of the compound. As shown in *Fig*. 2, W-H analysis was carried out to obtain the slope and y-intercept used to calculate the crystallite sizes of samples **1** and **2**. The crystallite sizes calculated by the W-H plot are about 6.2 nm and 12.6 nm, respectively. Even though the size difference of **2** in both calculations is larger than that of **1**, this difference is common in the methods. The crystallite size of **2** is larger than that of **1** in both methods.

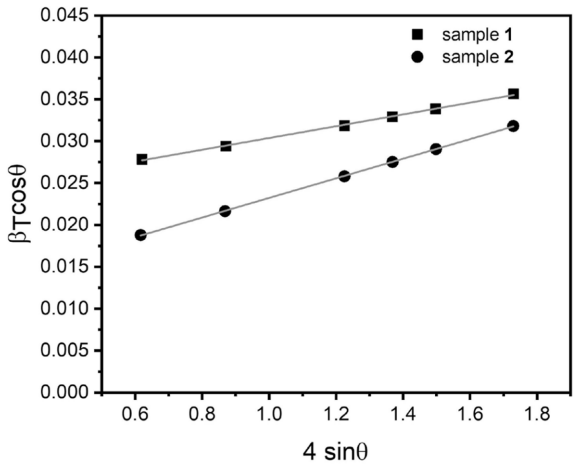

***Figure* 2.** Williamson-Hall (W-H) plots of sample **1** (filled squares) and **2** (filled circles), respectively.

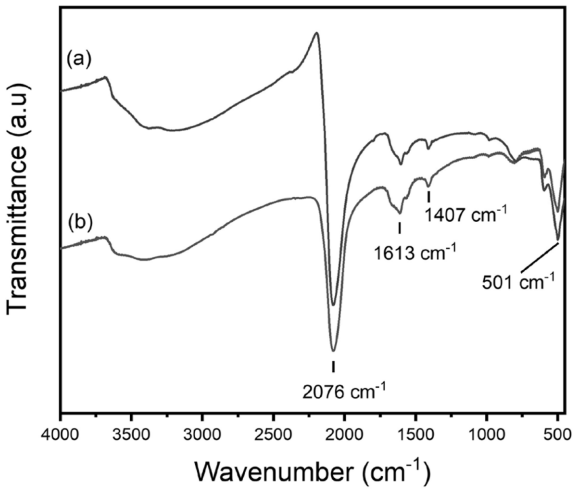

***Figure* 3.** FT-IR spectra of (a) sample **1** and (b) sample **2** in KBr pellet, respectively.

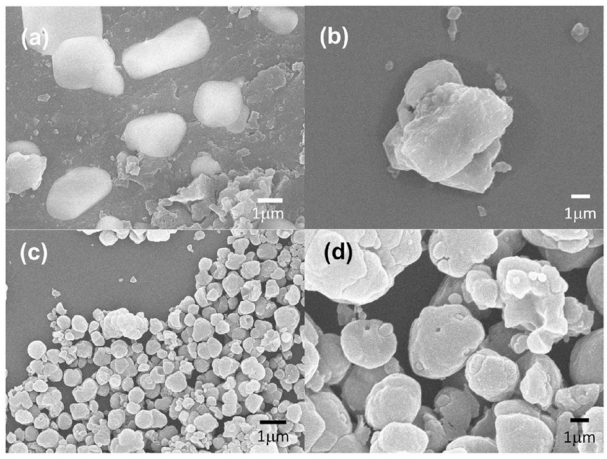

***Figure* 4.** SEM images of (a) and (b) sample **1**, and (c) and (d) sample **2**, respectively.

To further confirm the synthesis of PB, Fourier transform infrared spectroscopy (FT-IR) experiments were performed. FT-IR spectra can provide information concerning the vibrational frequencies of CN (ν_{CN}), which are strongly influenced by connectivity between metal ions and cyano ligands. *Fig*. 3 shows that the peak at 2076 cm^{-1} has a broad shape, which also supports the presence of Fe^{II}-C≡N-Fe^{III} in the products ($Fe_4[Fe(CN)_6]_3 \cdot xH_2O$).[19]

The SEM images indicate that the particles of the product are too nanocrystalline to observe the typical cubic particles of PB, a feature commonly seen in highly crystalline PB. Instead, aggregated spherical particles are observed in the SEM images, as shown in *Fig*. 4. These are presumed to be an agglomeration of nanocrystalline PB particles, consistent with the findings in the XRD analyses. Based on the above data, it is inferred from the SEM images and XRD pattern that even if the particles are large, they are composed of nanocrystalline materials.

To check the effect of the molar ratio of reactants on the final product, a reaction with the reactant ratio of 1:6.6 corresponding to 1.1 eq. of 1:6 (sample **3**) was examined. The XRD pattern of the product is quite different from those of samples **1** and **2**. The pattern was matched with the known compounds and revealed that the pattern corresponds to a mixture of potassium hexacyanoferrate(II) ($K_4Fe(CN)_6$) (JCPDS No. 00-001-0877),[20] potassium cyanide (KCN) (JCPDS No. 01-080-0102),[21] and potassium chloride (KCl) (JCPDS No. 00-041-1476),[22] as can be seen in *Fig*. 5. Therefore, the reaction equation of the reaction can be written as follows:

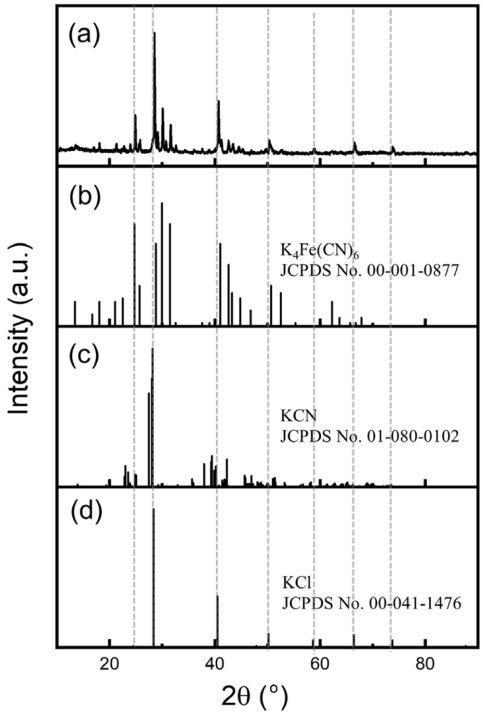

***Figure* 5.** (a) XRD pattern of sample **3** and peak assignment of (b) $K_4Fe(CN)_6$ (JCPDS No.: 00-001-0877), (c) KCN (JCPDS No.: 01-080-0120), and (d) KCl (JCPDS No. 00-041-1476) from top to bottom.

$$FeCl_2(s) + 6.6\ KCN(s) \rightarrow K_4Fe(CN)_6(s) + 0.6\ KCN(s) + 2\ KCl(s) \quad (4)$$

The formation of potassium hexacyanoferrate(II) could be also confirmed by the FT-IR spectrum, as shown in *Fig*. 6. The peak at 2047 cm^{-1} could be assigned as the CN vibrational frequency of CN^- (ν_{CN}) in potassium hexacyanoferrate(II).[23] This observation is quite remarkable in that

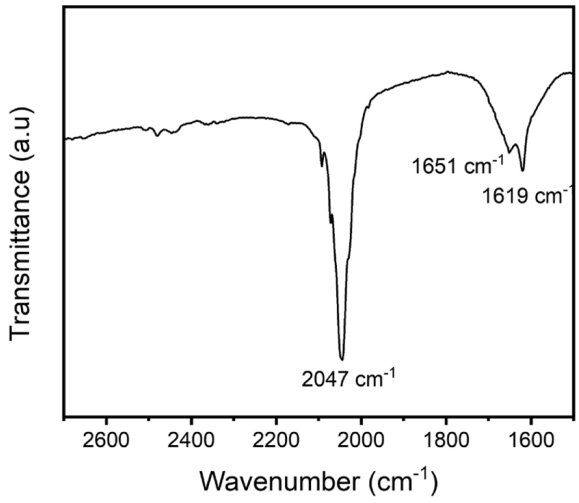

***Figure* 6.** FT-IR spectrum of the product in sample **3** in KBr pellet.

the final product is controlled by the choice of molar ratio of the reactants in the solid-state reaction. The more thermodynamically stable PB, as evidenced by the high lattice energy of PB,[24] is not generated and the kinetic product $K_4Fe(CN)_6$ is finally formed.

CONCLUSION

In summary, the application of the ball-milling technique, adopting a *de novo* approach for obtaining PB from the fundamental precursors of Fe^{2+} and CN^- ions with a carefully chosen molar ratio of reactants, presents a promising method for the solid-state synthesis of PB. Utilizing iron(II) chloride and potassium cyanide in a molar ratio of 1:2.8 yields PB, the desired product exhibiting high purity, a uniform particle size distribution, and significant nanocrystallinity. Crucially, the product yield was nearly quantitative at room temperature, underscoring the efficiency of the solid-state synthetic method. The effect of the molar ratio of reactants on the final product was also investigated, revealing significant differences in the case of sample **3**, where the Fe^{2+}:CN^- ratio was 1:6.6, resulting in a mixture of $K_4Fe(CN)_6$, KCN, and KCl. It is anticipated that this approach will contribute to a more environmentally friendly synthesis of PB and be employed for creating various advanced materials, especially in the cathode materials of lithium-ion and sodium-ion batteries using multimetallic PBAs with maximum entropy in the future. Nevertheless, further investigation is required to examine the impacts of ball-mill rpm, reaction time, and the quantity of added HCl on the resulting product. Our ongoing efforts are dedicated to advancing research in this direction.

Acknowledgments. Publication cost of this paper was supported by the Korean Chemical Society.

REFERENCES

1. Andreas Ludi *J. Chem. Educ.* **1981**, *58*, 1013.
2. Matos-Peralta Y.; Antuch, M. *J. Electrochem. Soc.* **2020**, *167*, 037510.
3. El-Mously, D. A.; Mahmoud, A. M.; Abdel-Raoof, A. M.; Elgazzar, E. *ACS Omega* **2022**, *7*, 43139.
4. Zaręba, J. K.; Szeremeta, J.; Waszkielewicz, M.; Nyk, M.; Samoć M. *Inorg. Chem.* **2016**, *55*, 9501.
5. Shatruk, M.; Dragulescu-Andrasi, A.; Chambers, K. E.; Stoian, S. A.; Bominaar, E. L.; Achim, C.; Dunbar K. R. *J. Am. Chem. Soc.* **2007**, *129*, 6104.
6. Yan, N.; Hu, L.; Li, Y.; Wang, Y.; Zhong, H.; Hu, X.; Kong, X.; Chen, Q. *J. Phys. Chem. C* **2012**, *116*, 7227.
7. Gao, Y.; Liu, H.; Zheng, Z.; Luan, X.; Xue, Y.; Li, Y. *NPG Asia Mater.* **2023**, *15*, 12.
8. Ding, Y.; Hu, Y.-L.; Gu, G.; Xia, X.-H. *J. Phys. Chem. C* **2009**, *113*, 14838
9. Hu, M.; Belik, A. A.; Imura, M.; Yamauchi, Y. *J. Am. Chem. Soc.* **2013**, *135*, 384
10. Jeon, Y.; Choi, K.; Im, S. *Bull. Korean Chem. Soc.* **2015**, *36*, 2966.
11. Jeon, Y.; Choi, K.; Im, S. *Bull. Korean Chem. Soc.* **2015**, *36*, 2970.
12. Brown, D. B.; Shriver, D. F. *Inorg. Chem.* **1969**, *8*, 37.
13. Jiang, W.; Wang, T.; Chen, H.; Suo, X.; Liang, J.; Zhu, W.; Li, H.; Dai, S. *Nano Energy* **2021**, *79*, 105464.
14. Peng, J.; Gao, Y.; Zhang, H.; Liu, Z.; Zhang, W.; Li, L.; Qiao, Y.; Yang, W.; Wang, J.; Dou, S.; Chou S. *Angew. Chem. Int. Ed.* **2022**, *61*, e202205867.
15. Luo, Y.; Peng, J.; Yin, S.; Xue, L.; Yan, Y. *Nanomaterials* **2022**, *12*, 1290.
16. He, S.; Zhao, J.; Rong, X.; Xu, C.; Zhang, Q.; Shen, X.; Qi, X.; Li, Y.; Li, X.; Niu, Y.; Li, X.; Han, S.; Gu, L.; Liu, H.; Hu, Y.-S. *Chem. Eng. J.* **2022**, *428*, 131083.
17. Herren, F.; Fischer, P.; Ludi, A.; Haelg, W. *Inorg. Chem.* **1980**, *19*, 956.
18. Debye, P.; Scherrer, P. *Physik. Z.* **1916**, *17*, 277.
19. Suryanarayana, C.; Grant Norton, M. X-ray Diffraction: A Practical Approach. Springer, 1998, New York.
20. Ayers, J. B.; Waggoner, W. H. *J. Inorg. Nucl. Chem.* **1971**, *33*, 721.
21. Hanawalt, J. D.; Rinn, H. W.; Frevel, L. K. *Ind. Eng. Chem. Anal. Ed.* **1938**, *10*, 457.
22. Stokes, H. T.; Decker, D. L.; Nelson, H. M.; Jorgensen, J. D. *Phys. Rev. B: Condens. Matter* **1993**, *47*, 11082.
23. Copper, M. J.; Rouse, K. D. *Acta Cryst.* **1973**, *A29*, 514
24. Penche, G.; González-Marcos, M. P.; González-Velasco, J. R. *Top. Catal.* **2022**, *65*, 1541.
25. Rosseinsky, D. R.; Glasser, L.; Jenkins, H. D. B. *J. Am. Chem. Soc.* **2004**, *126*, 10472.